

An Efficient Predistorter Design for Compensating Nonlinear Memory High Power Amplifiers

Sheng Chen, *Fellow, IEEE*

Abstract—This contribution applies digital predistorter to compensate distortions caused by memory high power amplifiers (HPAs) which exhibit true output saturation characteristics. Particle swarm optimization is first implemented to identify the Wiener HPA's parameters. The estimated Wiener HPA model is then directly used to design the predistorter. The proposed digital predistorter solution is attractive owing to its low on-line computational complexity, small memory units required and simple VLSI hardware structure implementation. Moreover, the designed predistorter is capable of successfully compensating serious nonlinear distortions and memory effects caused by the memory HPA operating in the output saturation region. Simulation results obtained are presented to demonstrate the effectiveness of this novel digital predistorter design.

Index Terms—Hammerstein model, memory high power amplifier, output saturation, particle swarm optimization, predistorter, Wiener model.

I. INTRODUCTION

HIGH POWER AMPLIFIER (HPA) is an indispensable component for any wireless communication system. To achieve high energy-efficiency, HPAs should operate at their output saturation regions but this operational mode could not accommodate high bandwidth-efficiency single-carrier high-order quadrature amplitude modulation (QAM) signals [1] as well as multi-carrier orthogonal frequency division multiplexing (OFDM) signals [2]. Even with a signal of low power envelope fluctuations, the nonlinearities of HPA may introduce distortions, causing adjacent channel interference and degrading the system's bit error rate (BER) performance. It is therefore critical to compensate the nonlinearity of the HPA in the design of a wireless system. In the early researches, HPAs were often considered to be memoryless. However, for high-rate broadband signals, the influence of the HPAs' memory effects can no longer be ignored. The memory effects are mostly caused by electrical or electrothermal factors which are elaborated in [3]. An accurate linearized compensation technique therefore needs to consider not only the nonlinearities caused by the current input signals but also the distortion

induced by the memory effects. Of all the linearization techniques, digital baseband predistorter (PD) is considered the most effective because it offers a modest implementation cost, while achieves a relatively good performance.

Many predistortion techniques [4]–[17] have been proposed to correct the distortions caused by the nonlinearity as well as the memory effect of memory HPAs. The look-up table (LUT) based techniques [4]–[6] realize a PD by representing the inverse characteristic function of the memory HPA in a LUT. The so-called indirect-learning based PD designs [10]–[12] first identify a post-inverse polynomial filter for the memory HPA to be compensated and then copy the post-inverse polynomial filter to form the PD. By contrast, the direct-learning based PD designs [13]–[15] first identify the input-output relation of the memory HPA using a polynomial model and then adapt a polynomial PD directly to invert the resulting polynomial HPA model. A recent work [16] uses a neural-fuzzy based PD, instead of a polynomial based PD, in the indirect-learning structure. The work [17] presents an interesting algebraic PD solution based directly on the Wiener HPA model parameters. However, the design of [17] is incomplete, and the solution is invalid for memory HPAs operating into the saturation region. Moreover, the authors of [17] assume that the Wiener HPA model parameters are known exactly and can directly be used for the algebraic based PD design, which is unrealistic.

It is well understood that the memory HPA can be modeled by the Wiener model consisting of a linear filter followed by a memoryless nonlinearity [18]. Physically, the memoryless nonlinearity of the HPA is represented by the output amplitude and phase response functions that are the nonlinear functions of the input signal amplitude. Most of the researches, including [10]–[17], adopt a two-parameters output amplitude response model [19], which peaks at an input saturation amplitude. However, when the input amplitude increases beyond this saturation point, the output amplitude of this model actually starts to fall. This is in contrast to the physical intuition that the output amplitude should not fall off beyond saturation as is supported by the real measurements of HPAs [18].

Against this background and motivated by the work [17], a novel PD design is proposed based on a direct learning structure in this contribution. The parameters of the Wiener HPA model are first identified using a particle swarm optimization (PSO) algorithm [20]. PSO [20] is an efficient population-based stochastic global optimization technique inspired by social behavior of bird flocks or fish schools, and it has been successfully applied to wide-ranging optimization applications [21]–[27]. Owing to the effectiveness of PSO, an accurate Wiener HPA model can be obtained, based on which an algebraic based PD

Manuscript received March 29, 2011; revised August 01, 2011; accepted August 03, 2011. Date of publication September 26, 2011; date of current version November 23, 2011.

The author is with the School of Electronics and Computer Science, University of Southampton, Southampton SO17 1BJ, U.K. (e-mail: sqc@ecs.soton.ac.uk).

Color versions of one or more of the figures in this paper are available online at <http://ieeexplore.ieee.org>.

Digital Object Identifier 10.1109/TBC.2011.2165008

solution can readily be derived. This is in contrast to polynomial PD designs, which require expensive on-line adaptation process as well as large number of storage units. Therefore, our proposed PD enjoys a low computational cost. Furthermore, it exhibits a natural pipeline data processing structure which enables a simple VLSI hardware implementation. Although in this contribution, we consider single-carrier QAM systems, our approach is equally applicable to multi-carrier OFDM systems. We now summarize our novel contributions in comparison with the work [17].

- 1) The work [17] employs a memory HPA model where the output amplitude continues to fall off after saturation, while we adopt a more realistic memory HPA model which exhibit true output saturation characteristics.
- 2) Unlike [17] which assumes the exact Wiener HPA parameters in obtaining the PD solution, we identify the parameters of the Wiener HPA model using the efficient PSO algorithm, and obtain the PD solution using the estimated Wiener HPA model.
- 3) The algebraic based PD solution presented in [17] is incomplete. In fact, it is invalid for memory HPAs that operate into the saturation region. By contrast, our PD solution is properly designed and is capable of successfully compensating serious saturation distortions caused by the memory HPA operating in the output saturation region.

The rest of this contribution is organized as follows. The Wiener model for memory HPAs is introduced in Section II, where the PSO algorithm is also presented for an accurate identification of the Wiener HPA model. In Section III, the proposed PD solution is detailed. The pipeline processing structure of the proposed PD solution is also briefly outlined, which enables an efficient VLSI hardware implementation of the PD. Simulation results are presented in Section IV to demonstrate the effectiveness of the proposed PD design approach, while our conclusions are drawn in Section V.

II. MEMORY HIGH POWER AMPLIFIER MODEL

In order to construct an effective PD, it is critical to find an appropriate HPA model. A widely used model for memory HPAs is the Wiener model [18]. The Wiener model comprises a linear system followed by a memoryless nonlinearity. An advantage of adopting the Wiener model for PD design is that the exact inverse system of the Wiener model can be represented by a memoryless nonlinearity followed by a linear system, which is known as the Hammerstein model.

A. Wiener Model for Memory HPAs

The Wiener HPA model consists of a linear filter followed by a memoryless nonlinearity [18]. The linear filter of order N_h represents the memory effect on the input signal, and its z transfer function is defined by

$$H(z) = \sum_{i=0}^{N_h} h_i z^{-i}, \quad (1)$$

while the linear filter coefficient vector is given by

$$\mathbf{h} = [h_0 \ h_1 \ \cdots \ h_{N_h}]^T. \quad (2)$$

Given the input signal $x(k)$ to the memory HPA, the unobservable linear filter output

$$w(k) = \sum_{i=0}^{N_h} h_i x(k-i), \quad (3)$$

is the input to the memoryless nonlinearity part of the HPA model which we assume to be the travelling-wave tube (TWT) nonlinearity [18], [19]. The baseband complex-valued input signal $w(k)$ to the TWT nonlinearity can be expressed as

$$w(k) = |w(k)| \cdot \exp(j\angle w(k)) = r_w(k) \cdot \exp(j\psi(k)), \quad (4)$$

where $r_w(k) = |w(k)|$ denotes the amplitude of $w(k)$ and $\psi(k) = \angle w(k)$ its phase.

As the signal travels through the TWT nonlinearity, it is affected by the nonlinear amplitude as well as phase functions of the HPA, and the output signal $y(k)$ is distorted mainly depending on the input signal amplitude $r_w(k)$, yielding

$$y(k) = |y(k)| \cdot \exp(j\angle y(k)) = A(r_w(k)) \cdot \exp(j(\psi(k) + \Phi(r_w(k)))). \quad (5)$$

The output amplitude $A(r_w(k))$ and the phase $\Phi(r_w(k)) = \angle y(k) - \psi(k)$ of the HPA are specified respectively by¹

$$A(r) = \begin{cases} \frac{\alpha_a r}{1 + \beta_a r^2}, & 0 \leq r \leq r_{\text{sat}}, \\ A_{\text{max}}, & r > r_{\text{sat}}, \end{cases} \quad (6)$$

$$\Phi(r) = \frac{\alpha_\phi r^2}{1 + \beta_\phi r^2}, \quad (7)$$

with the parameter vector that specifies the TWT nonlinearity given by

$$\mathbf{t} = [\alpha_a \ \beta_a \ \alpha_\phi \ \beta_\phi]^T, \quad (8)$$

where the saturating input amplitude is defined as

$$r_{\text{sat}} = \frac{1}{\sqrt{\beta_a}}, \quad (9)$$

while the saturation output amplitude is given by

$$A_{\text{max}} = \frac{\alpha_a}{2\sqrt{\beta_a}}. \quad (10)$$

¹Most works assume an output amplitude $A(r) = \alpha_a r / (1 + \beta_a r^2)$, which peaks at $r = r_{\text{sat}}$ but falls off from the peak value A_{max} when $r > r_{\text{sat}}$. This is against the physical intuition that the output amplitude should not fall off beyond saturation. Our output amplitude model (6) is more realistic and is supported by the real measurements of HPAs [18].

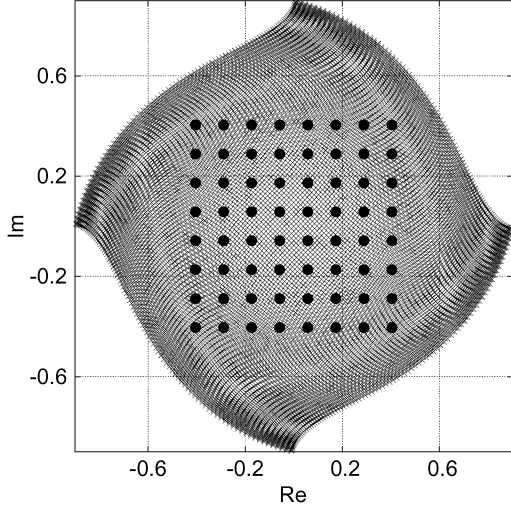


Fig. 1. Output $y(k)$, marked by \times , of the memory HPA for the 64-QAM input signal $x(k)$, marked by \bullet , where the memory HPA, specified by $\mathbf{h}^T = [0.76920.15380.0769]$ and $\mathbf{t}^T = [2.15871.154.02.1]$, is operating at the IBO of 10 dB.

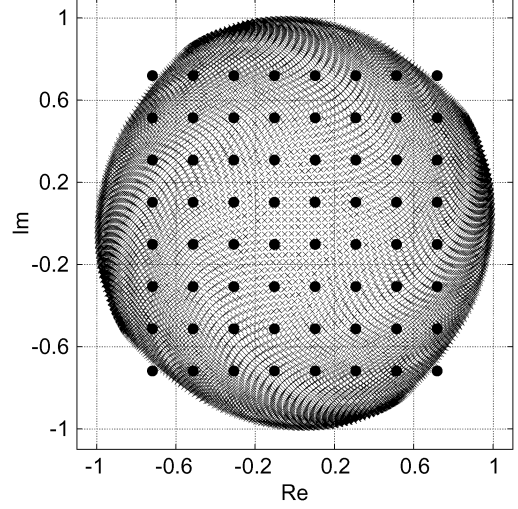


Fig. 2. Output $y(k)$, marked by \times , of the memory HPA for the 64-QAM input signal $x(k)$, marked by \bullet , where the memory HPA, specified by $\mathbf{h}^T = [0.76920.15380.0769]$ and $\mathbf{t}^T = [2.15871.154.02.1]$, is operating at the IBO of 5 dB.

Note that the underlying physics requires that $A_{\max} > r_{\text{sat}}$.

We define the input back-off (IBO) of the HPA as

$$\text{IBO} = 10 \cdot \log_{10} \frac{P_{\text{sat}}}{P_{\text{avg}}}, \quad (11)$$

where $P_{\text{sat}} = r_{\text{sat}}^2$ is the saturation input power and P_{avg} is the average power of the signal at the input of the TWT nonlinearity. Note that P_{avg} is defined as the average power of $w(k)$, which is equal to the average power of the memory HPA's input $x(k)$ scaled by the linear filter power gain $\|\mathbf{h}\|^2$. Consider the memory HPA specified by

$$\begin{aligned} \mathbf{h}^T &= [0.7692 \quad 0.1538 \quad 0.0769], \\ \mathbf{t}^T &= [2.1587 \quad 1.15 \quad 4.0 \quad 2.1]. \end{aligned} \quad (12)$$

For the 64-QAM signal $x(k)$, Figs. 1 and 2 plot the output signals $y(k)$ of the memory HPA for the IBO values of 10 dB and 5 dB, respectively, where the serious distortions caused by the memory HPA can be clearly seen. Moreover, it can be seen from Fig. 2 that the memory HPA is operating into the output saturation region of $r > r_{\text{sat}}$ in the case of IBO = 5 dB.

B. Identification of the Wiener HPA Model With PSO

Given a block of training data $\{\mathbf{x}(k), y(k)\}_{k=1}^K$, where $\mathbf{x}(k) = [x(k)x(k-1)\cdots x(k-N_h)]^T$, the task is to estimate the true parameter vector of the memory HPA, defined as

$$\boldsymbol{\theta} = [\mathbf{h}^T \quad \mathbf{t}^T]^T = [\theta_1 \quad \theta_2 \cdots \theta_{N_\theta}]^T, \quad (13)$$

where $N_\theta = N_h + 5$. The measured memory HPA's output may be corrupted by the small noise and, therefore, it takes the form

$$y(k) = F_{\text{HPA}}(\mathbf{x}(k); \boldsymbol{\theta}) + \mu(k), \quad (14)$$

where the complex-valued nonlinear mapping $F_{\text{HPA}}(\bullet; \boldsymbol{\theta})$ is specified by (3)–(7), while $\mu(k)$ is the complex-valued Gaussian white noise with $E[|\mu(k)|^2] = 2\sigma_\mu^2$. The Wiener model output with the parameter estimate $\tilde{\boldsymbol{\theta}}$ is expressed by

$$\tilde{y}(k) = F_{\text{HPA}}(\mathbf{x}(k); \tilde{\boldsymbol{\theta}}). \quad (15)$$

Let the error between the desired output $y(k)$ and the model output $\tilde{y}(k)$ be defined as $e(k) = y(k) - \tilde{y}(k)$, yielding the mean square error (MSE) cost function

$$J(\tilde{\boldsymbol{\theta}}) = \frac{1}{K} \sum_{k=1}^K |e(k)|^2. \quad (16)$$

The estimate of the true parameter vector $\boldsymbol{\theta}$ is then defined as the solution of the following optimization

$$\hat{\boldsymbol{\theta}} = \arg \min_{\tilde{\boldsymbol{\theta}} \in \Theta} J(\tilde{\boldsymbol{\theta}}), \quad (17)$$

where the search space is specified by

$$\Theta \triangleq \prod_{i=1}^{N_\theta} [\theta_{i,\min}, \theta_{i,\max}], \quad (18)$$

and the true parameter vector $\boldsymbol{\theta} \in \Theta$. The cost function (16) is highly nonlinear and may contain local minima. Therefore, conventional gradient-based estimators [28], [29] require a good initial parameter estimate in order to avoid local minima, which may be difficult to guarantee in practice. We use the PSO to solve this challenging identification problem.

When applying a PSO [20] to solve the optimization (17), a swarm of particles $\{\tilde{\boldsymbol{\theta}}^l(m)\}_{m=1}^S$ are “flying” in the search space Θ in order to find a solution $\hat{\boldsymbol{\theta}}$, where S is

the size of the swarm and $l \in \{0, 1, \dots, L_{\max}\}$ denotes the l th movement of the swarm. Each particle position $\tilde{\boldsymbol{\theta}}(m) = [\tilde{\theta}_1(m) \tilde{\theta}_2(m) \dots \tilde{\theta}_{N_\theta}(m)]^T$ has a N_θ -dimensional velocity $\mathbf{v}(m) = [v_1(m) v_2(m) \dots v_{N_\theta}(m)]^T$ to direct its search, and $\mathbf{v}(m) \in \mathbf{V}$ with the velocity space defined by

$$\mathbf{V} \triangleq \prod_{i=1}^{N_\theta} [-v_{i,\max}, v_{i,\max}], \quad (19)$$

where $v_{i,\max} = (1/2)(\theta_{i,\max} - \theta_{i,\min})$.

To start the PSO, the particles $\{\tilde{\boldsymbol{\theta}}^0(m)\}_{m=1}^S$ are initialized randomly within Θ , and the velocity for each candidate particle is initialized to zero, namely, $\{\mathbf{v}^0(m) = \mathbf{0}\}_{m=1}^S$. The cognitive information $\mathbf{pb}^l(m)$ and the social information \mathbf{gb}^l record the best position visited by the particle m and the best position visited by the entire swarm, respectively, during the l movements. The MSE costs associated with $\mathbf{pb}^l(m)$ and \mathbf{gb}^l are given by $J(\mathbf{pb}^l(m))$ and $J(\mathbf{gb}^l)$, respectively. The cognitive information $\mathbf{pb}^l(m)$ and the social information \mathbf{gb}^l are used to update the velocities and positions according to

$$\begin{aligned} \mathbf{v}^{l+1}(m) = & I_w \cdot \mathbf{v}^l(m) + \text{rand}() \cdot c_1 \cdot (\mathbf{pb}^l(m) - \tilde{\boldsymbol{\theta}}^l(m)) \\ & + \text{rand}() \cdot c_2 \cdot (\mathbf{gb}^l - \tilde{\boldsymbol{\theta}}^l(m)), \end{aligned} \quad (20)$$

$$\tilde{\boldsymbol{\theta}}^{l+1}(m) = \tilde{\boldsymbol{\theta}}^l(m) + \mathbf{v}^{l+1}(m), \quad (21)$$

where I_w denotes the inertia weight, $\text{rand}()$ is the random number uniformly distributed in $[0, 1]$, c_1 and c_2 are the two acceleration coefficients. Experimental results given in [25] show that a better performance can be achieved by using $I_w = \text{rand}()$ instead of a constant inertia weight. Adopting the time varying acceleration coefficients (TVAC) [22], in which

$$\begin{aligned} c_1 &= 2.5 - (2.5 - 0.5) \cdot l/L_{\max}, \\ c_2 &= 0.5 + (2.5 - 0.5) \cdot l/L_{\max}, \end{aligned} \quad (22)$$

can often enhance the performance of PSO. The search space Θ and the velocity space \mathbf{V} are used to confine $\tilde{\boldsymbol{\theta}}^{l+1}(m)$ and $\mathbf{v}^{l+1}(m)$ derived from (20) and (21), respectively. If $\mathbf{v}^{l+1}(m) = \mathbf{0}$, it is randomly re-initialized to a non-zero value inside \mathbf{V} . The detailed PSO algorithm is summarized as follows.

a) *PSO initialization:*

Specify the swarm size S and the number of iterations L_{\max}

Randomly initialize $\{\tilde{\boldsymbol{\theta}}^0(m)\}_{m=1}^S$ in Θ , and set $\{\mathbf{v}^0(m) = \mathbf{0}\}_{m=1}^S$

Compute the MSE costs $\{J(\tilde{\boldsymbol{\theta}}^0(m))\}_{m=1}^S$, set $\{\mathbf{pb}^0(m) = \tilde{\boldsymbol{\theta}}^0(m)\}_{m=1}^S$ and

$$\mathbf{gb}^0 = \arg \min_s \{J(\tilde{\boldsymbol{\theta}}^0(m))\}_{m=1}^S$$

b) *PSO evolution:*

for ($l = 0; l < L_{\max}; l++$) {

for ($m = 1; m \leq S; m++$) {

Calculate $\mathbf{v}^{l+1}(m)$ according to (20)

for ($i = 1; i \leq N_\theta; i++$) {

If $v_i^{l+1}(m) = 0$: $v_i^{l+1}(m) = \pm 0.5 \cdot \text{rand}() \cdot v_{i,\max}$

If $v_i^{l+1}(m) > v_{i,\max}$: $v_i^{l+1}(m) = v_{i,\max}$

If $v_i^{l+1}(m) < -v_{i,\max}$: $v_i^{l+1}(m) = -v_{i,\max}$

}

Calculate $\tilde{\boldsymbol{\theta}}^{l+1}(m)$ according to (21)

for ($i = 1; i \leq N_\theta; i++$) {

If $\tilde{\theta}_i^{l+1}(m) > \theta_{i,\max}$: $\tilde{\theta}_i^{l+1}(m) = \theta_{i,\max}$

If $\tilde{\theta}_i^{l+1}(m) < \theta_{i,\min}$: $\tilde{\theta}_i^{l+1}(m) = \theta_{i,\min}$

}

Compute $J(\tilde{\boldsymbol{\theta}}^{l+1}(m))$

$\mathbf{pb}^{l+1}(m) = \mathbf{pb}^l(m)$

If $J(\mathbf{pb}^{l+1}(m)) > J(\tilde{\boldsymbol{\theta}}^{l+1}(m))$: $\mathbf{pb}^{l+1}(m) = \tilde{\boldsymbol{\theta}}^{l+1}(m)$

If $J(\mathbf{gb}^l) > J(\mathbf{pb}^{l+1}(m))$: $\mathbf{gb}^l = \mathbf{pb}^{l+1}(m)$

}

$\mathbf{gb}^{l+1} = \mathbf{gb}^l$

}

c) *PSO termination:*

The solution is $\hat{\boldsymbol{\theta}} = \mathbf{gb}^{L_{\max}}$

III. PROPOSED PREDISTORTER DESIGN

Basically for the Wiener HPA model, the corresponding PD should be the inverse of the Wiener model, which is a Hammerstein model consisting of a memoryless nonlinearity followed by a linear memory filter. More specifically, the memoryless nonlinearity of the Hammerstein PD should invert the memoryless nonlinearity of the Wiener HPA, while the linear filter of the Hammerstein PD should invert the linear filter of the Wiener HPA.

A. Algebraic Solution for Predistorter

Let the transfer function of the Hammerstein PD's linear filter be

$$G(z) = z^{-\tau} \cdot \sum_{i=0}^{N_g} g_i z^{-i}, \quad (23)$$

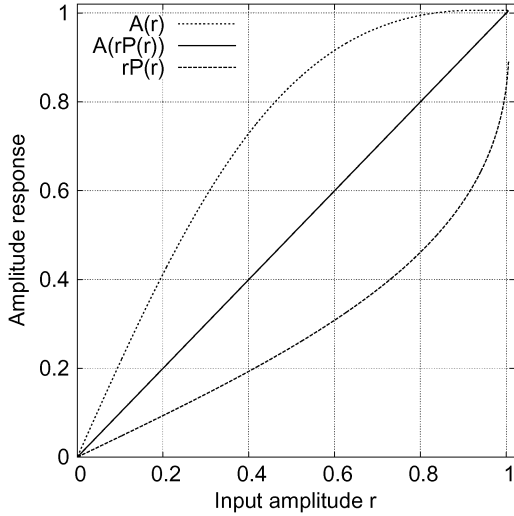


Fig. 3. HPA's amplitude response function $A(r)$, the amplitude predistortion function $r \cdot P(r)$ of the PD, and the combined amplitude response function $A(r \cdot P(r))$ of the PD and HPA over the range of $0 \leq r \leq A_{\max}$, where the HPA's parameters $\alpha_a = 2.1587$ and $\beta_a = 1.15$.

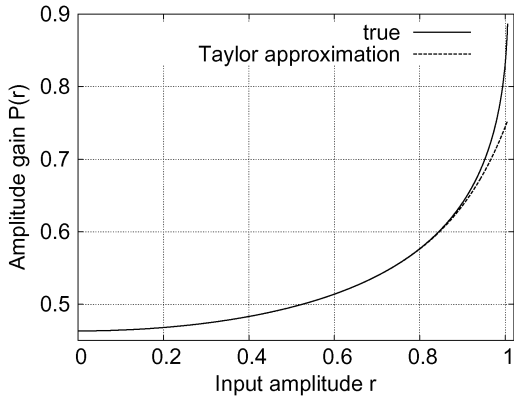


Fig. 4. Amplitude gain $P(r)$ of the PD and its Taylor approximation $\hat{P}(r)$ with $N_t = 9$ over the range of $0 \leq r \leq A_{\max}$, where the HPA's parameters $\alpha_a = 2.1587$ and $\beta_a = 1.15$.

where the delay $\tau = 0$ if $H(z)$ is minimum phase. The solution of the PD's linear filter $\mathbf{g} = [g_0 g_1 \cdots g_{N_g}]^T$ can readily be obtained by solving the set of linear equations specified by

$$G(z) \cdot H(z) = z^{-\tau}. \quad (24)$$

To guarantee an accurate inverse, the length of \mathbf{g} should be chosen to be two to three times of the length of \mathbf{h} .

The memoryless nonlinearity of the PD should introduce the appropriate amplitude and phase predistortion functions that can compensate the nonlinear amplitude and phase functions of the HPA's nonlinearity, as described by (6) and (7). Again denote the amplitude of the input signal $x(k)$ by $r(k) = |x(k)|$. Let us define the amplitude gain function of the PD's nonlinearity by $P(r)$, which means that the amplitude predistortion function of this memoryless nonlinearity is $r \cdot P(r)$, and the corresponding phase predistortion function by $\Omega(r)$. Noting (6), the required

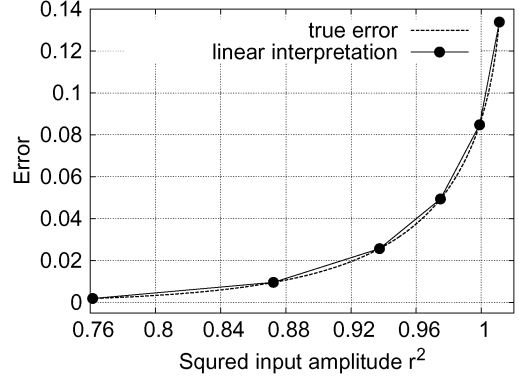


Fig. 5. Error between the amplitude gain $P(r)$ and the Taylor approximation $\hat{P}(r)$ with $N_t = 9$ as well as its 5-piecewise linear interpretation over the region $(\hat{R}_0^2, \hat{R}_5^2]$ with $\hat{R}_5 = A_{\max}$, where the HPA's parameters $\alpha_a = 2.1587$ and $\beta_a = 1.15$.

correction equation for the amplitude predistortion function to meet is²

$$A(r \cdot P(r)) = r, \quad \text{for } r \cdot P(r) \leq r_{\text{sat}}. \quad (25)$$

Joint considering (25) and (6) leads to

$$\beta_a r^2 \cdot P^2(r) - \alpha_a \cdot P(r) + 1 = 0, \quad \text{for } r \cdot P(r) \leq r_{\text{sat}}. \quad (26)$$

which has the two solutions, and the required amplitude gain function can be taken to be the smaller solution

$$P(r) = \frac{\alpha_a - \sqrt{\alpha_a^2 - 4\beta_a r^2}}{2\beta_a r^2}, \quad \text{for } r \leq A_{\max}. \quad (27)$$

Note that the solution (27) only has the meaning for $\alpha_a^2 - 4\beta_a r^2 \geq 0$, or $r \leq A_{\max}$. Furthermore, for this $P(r)$, $r \leq A_{\max}$ implies $r \cdot P(r) \leq r_{\text{sat}}$. When $r > A_{\max}$ or $r \cdot P(r) > r_{\text{sat}}$, it is impossible to meet the condition $A(r \cdot P(r)) = r$, because of the output saturation characteristics of (6). In this situation, one may simply set $P(r) = 1$. Thus, the appropriate amplitude gain function is

$$P(r) = \begin{cases} \frac{\alpha_a - \sqrt{\alpha_a^2 - 4\beta_a r^2}}{2\beta_a r^2}, & r \leq A_{\max}, \\ 1, & r > A_{\max}. \end{cases} \quad (28)$$

Noting (7), the required correction equation for the phase predistortion function to meet is

$$\Phi(r \cdot P(r)) + \Omega(r) = 0. \quad (29)$$

Based on (29) and (7), the solution of the phase predistortion function $\Omega(r)$ is given by

$$\Omega(r) = -\Phi(r \cdot P(r)) = -\frac{\alpha_\phi (r \cdot P(r))^2}{1 + \beta_\phi (r \cdot P(r))^2}. \quad (30)$$

This phase predistortion function is valid for any r .

²In the work [17], the correction equation (25) was mistaken to be valid for any value of r . Even with the unrealistic HPA's output amplitude function $A(r) = \alpha_a r / (1 + \beta_a r^2)$ that does not exhibit the true output saturation characteristics, the required amplitude gain function (27) only has the meaning for $r \leq A_{\max}$.

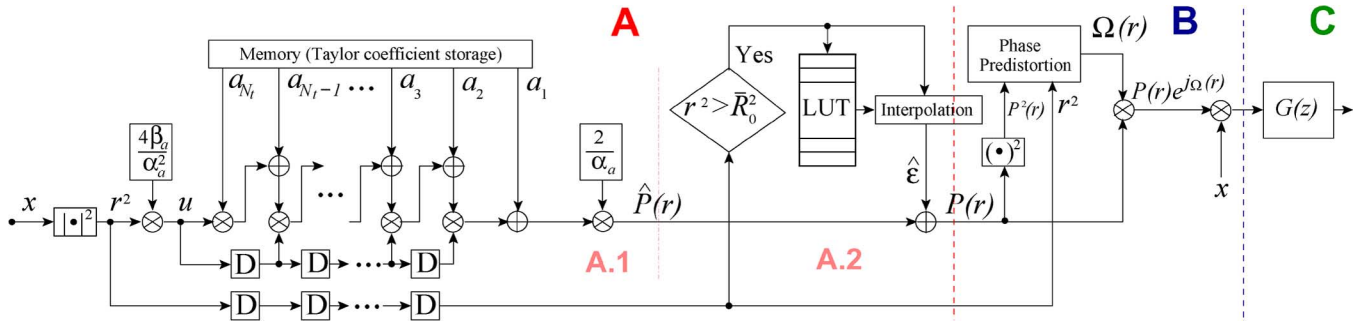


Fig. 6. VLSI structure of the proposed predistorter over the range of $r^2 \leq A_{\max}^2$. Note that for $r^2 > A_{\max}^2$, $P(r) = 1$.

TABLE I
ON-LINE COMPUTATIONAL COMPLEXITY FOR THE MEMORYLESS NONLINEAR
PREDISTORTION PART OF THE PROPOSED PD

operation	multiplications	additions
$r^2 = x ^2$	2	1
amplitude gain $\hat{P}(r)$ of (34)	N_t	$N_t - 1$
piecewise-linear error $\hat{\varepsilon}(r^2)$ of (36)	1	1
phase predistortion $\Omega(r)$ of (30)	5	1
total (with error compensation)	$N_t + 8$	$N_t + 3$

For the HPA's nonlinear amplitude response function (6) specified by $\alpha_a = 2.1587$ and $\beta_a = 1.15$, Fig. 3 plots the HPA's amplitude response function $A(r)$, the amplitude predistortion function $r \cdot P(r)$ with $P(r)$ given in (27), and the combined amplitude response function $A(r \cdot P(r))$ of the PD and HPA, for $0 \leq r \leq A_{\max}$.

The amplitude gain function (27) includes a square root calculation and division by r^2 . Division with r^2 may cause inaccurate results when the signal r^2 is close to zero, while square-root-free calculation is highly desired for a simple hardware implementation. For these reasons, the solution (27) is expanded with a Taylor series expansion. First let us define

$$\lambda = \frac{4\beta_a r^2}{\alpha_a^2}. \quad (31)$$

Expand $(1 - \lambda)^{1/2}$ around $\lambda = 0$ by the Taylor series

$$(1 - \lambda)^{\frac{1}{2}} = 1 - \sum_{i=1}^{N_t} a_i \lambda^i - \mathcal{O}(\lambda^{N_t+1}), \quad \text{for } \lambda \leq 1, \quad (32)$$

where a_i , $1 \leq i \leq N_t$, are positive constants and N_t is the order of Taylor expansion. Note that $\lambda \leq 1$ corresponds to $r^2 \leq A_{\max}^2$. Therefore, the amplitude gain function $P(r)$ of (27) can be expressed as

$$\begin{aligned} P(r) &= \frac{\alpha_a - \alpha_a(1 - \lambda)^{1/2}}{2\beta_a r^2} \\ &= \sum_{i=1}^{N_t} \frac{2a_i(4\beta_a)^{i-1}}{\alpha_a^{2i-1}} r^{2(i-1)} \\ &\quad + \mathcal{O}(r^{2N_t}), \quad \text{for } r \leq A_{\max}. \end{aligned} \quad (33)$$

Thus, the amplitude gain function $P(r)$ for $r^2 \leq A_{\max}^2$ can be approximated by

$$\hat{P}(r) = \sum_{i=1}^{N_t} \frac{2a_i}{\alpha_a} \left(\frac{4\beta_a}{\alpha_a^2} \right)^{i-1} (r^2)^{i-1}, \quad \text{for } r^2 \leq A_{\max}^2. \quad (34)$$

Fig. 4 depicts the amplitude gain $P(r)$ and its Taylor approximation $\hat{P}(r)$ with $N_t = 9$ over the range of $0 \leq r \leq A_{\max}$, where it can be seen that for $r > r_{\text{sat}}$ the approximation error $\mathcal{O}(r^{2N_t})$ is noticeable.

For the input signal with amplitude satisfying $r^2 < r_{\text{sat}}^2$, a small N_t is sufficient to guarantee a negligibly small residual $\mathcal{O}((r^2)^{N_t})$, and $\hat{P}(r)$ with $N_t = 9$ is very accurate. When the HPA operates in the highly saturated region of $r^2 \geq r_{\text{sat}}^2$, however, the resulting residual $\mathcal{O}((r^2)^{N_t})$ can no longer be ignored. In this case, increasing N_t to improve the accuracy of $\hat{P}(r)$ is inadvisable. This is because an overly large N_t not only imposes excessively high computational cost but also introduces inaccuracy when r^2 is very small. Furthermore, when N_t increases to beyond 9, the rate of reduction in the approximation error $\mathcal{O}((r^2)^{N_t})$ becomes very slow for $r^2 > r_{\text{sat}}^2$. The solution is to operate $\hat{P}(r)$ in the operation condition of $r_{\text{sat}}^2 < r^2$ and to adopt a piecewise linear interpretation, similar to the interpretation LUT scheme in digital modems [30], to correct $\hat{P}(r)$ when the HPA operates in the saturation region. Specifically, define the residual between the true amplitude gain function $P(r)$ of (27) and the approximate amplitude gain function $\hat{P}(r)$ of (34) by

$$\varepsilon(r^2) = P(r) - \hat{P}(r) = \mathcal{O}((r^2)^{N_t}), \quad \text{for } r^2 \leq A_{\max}^2. \quad (35)$$

A small LUT of $Q + 1$ points, $\{\bar{R}_q^2, \varepsilon(\bar{R}_q^2)\}_{q=0}^Q$, is computed, where $\bar{R}_Q^2 = A_{\max}^2$ and $\bar{R}_1^2 \approx r_{\text{sat}}^2$, while \bar{R}_0^2 is identified as the point at which $\varepsilon(\bar{R}_0^2) \approx 0$. The Q -piecewise linear interpretation of $\varepsilon(r^2)$ is adopted over the amplitude range of $(\bar{R}_0^2, \bar{R}_Q^2]$ as

$$\hat{\varepsilon}(r^2) = s_q \cdot r^2 + b_q, \quad \bar{R}_{q-1}^2 < r^2 \leq \bar{R}_q^2, \quad (36)$$

with

$$\begin{aligned} s_q &= \frac{\varepsilon(\bar{R}_q^2) - \varepsilon(\bar{R}_{q-1}^2)}{\bar{R}_q^2 - \bar{R}_{q-1}^2}, \\ b_q &= \frac{\varepsilon(\bar{R}_{q-1}^2) \bar{R}_q^2 - \varepsilon(\bar{R}_q^2) \bar{R}_{q-1}^2}{\bar{R}_q^2 - \bar{R}_{q-1}^2}, \end{aligned} \quad (37)$$

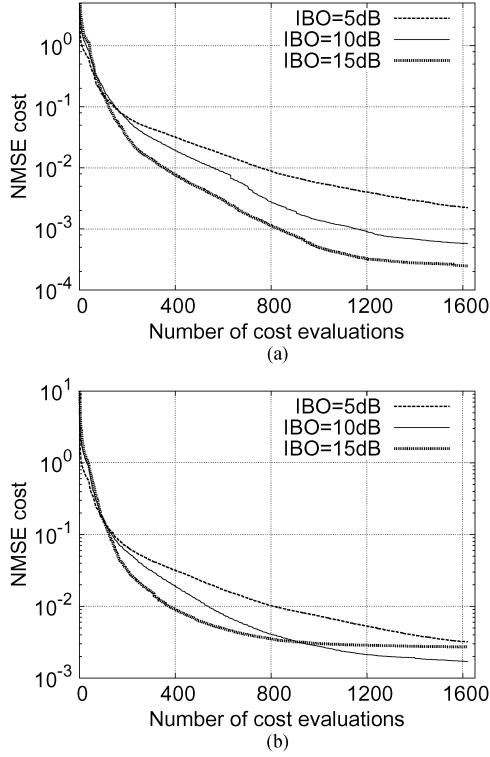


Fig. 7. Normalized MSE cost averaged over 100 runs as the function of number of cost evaluations for the PSO identification of the Wiener HPA: (a) the standard deviation of the measurement noise $\sigma_\mu = 0.0$, and (b) the standard deviation of the measurement noise $\sigma_\mu = 0.01$. The HPA's parameters are given in (12), while the PSO has the population size $S = 20$ with the number of iterations $L_{\max} = 80$.

TABLE II
PSO IDENTIFICATION RESULTS OF THE WIENER HPA

True HPA				
$\hat{\mathbf{h}}^T$	0.7692	0.1538	0.0769	
$\hat{\mathbf{t}}^T$	2.1587	1.15	4.0	2.1
Estimated HPA, $\sigma_\mu = 0$ and IBO= 5 dB				
$\hat{\mathbf{h}}^T$	0.77235	0.15472	0.07757	
$\hat{\mathbf{t}}^T$	2.14885	1.14122	3.95966	2.07337
Estimated HPA, $\sigma_\mu = 0$ and IBO= 10 dB				
$\hat{\mathbf{h}}^T$	0.77065	0.15413	0.07721	
$\hat{\mathbf{t}}^T$	2.15917	1.16780	3.97040	2.06925
Estimated HPA, $\sigma_\mu = 0$ and IBO= 15 dB				
$\hat{\mathbf{h}}^T$	0.77289	0.15442	0.07721	
$\hat{\mathbf{t}}^T$	2.14755	1.13908	3.97118	2.07126
Estimated HPA, $\sigma_\mu = 0.01$ and IBO= 5 dB				
$\hat{\mathbf{h}}^T$	0.76621	0.15156	0.07495	
$\hat{\mathbf{t}}^T$	2.14593	1.13209	4.03450	2.10592
Estimated HPA, $\sigma_\mu = 0.01$ and IBO= 10 dB				
$\hat{\mathbf{h}}^T$	0.76730	0.15320	0.07678	
$\hat{\mathbf{t}}^T$	2.16753	1.17666	4.03759	2.14617
Estimated HPA, $\sigma_\mu = 0.01$ and IBO= 15 dB				
$\hat{\mathbf{h}}^T$	0.77296	0.15422	0.07704	
$\hat{\mathbf{t}}^T$	2.15021	1.17551	4.00773	2.23344

where $\varepsilon(\bar{R}_0^2) = 0$ is assumed. Fig. 5 compares the true residual $\varepsilon(r^2)$ with its 5-piecewise linear interpretation $\hat{\varepsilon}(r^2)$.

In summary, the designed amplitude gain function is specified by

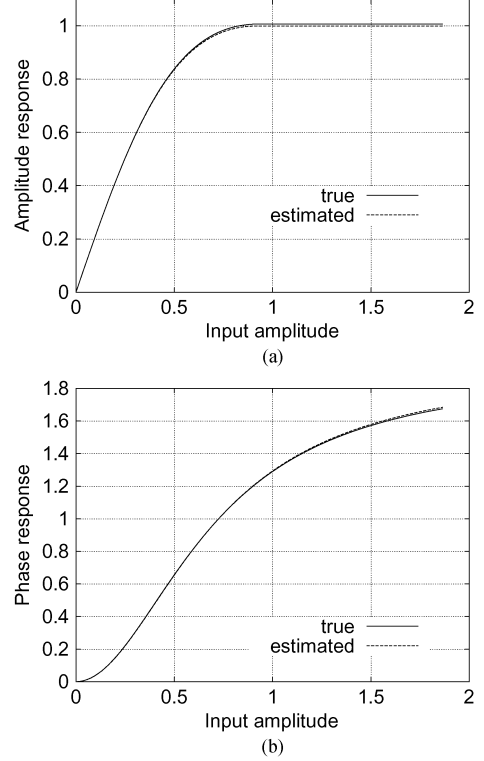


Fig. 8. Comparison of (a) the amplitude response and (b) the phase response between the static nonlinearity of the true Wiener HPA (12) and that of the estimated Wiener HPA model (43).

$$P(r) = \begin{cases} \hat{P}(r), & 0 \leq r^2 \leq \bar{R}_0^2, \\ \hat{P}(r) + \hat{\varepsilon}(r^2), & \bar{R}_{q-1}^2 < r^2 \leq \bar{R}_q^2, 1 \leq q \leq Q \\ 1, & r^2 > \bar{R}_Q^2 = A_{\max}^2, \end{cases} \quad (38)$$

where $\hat{P}(r)$ and $\hat{\varepsilon}(r^2)$ are given in (34) and (36), respectively, while the designed phase predistortion function $\Omega(r)$ is specified in (30).

B. Hardware Design and Computational Complexity

We now examine the VLSI structure for implementing the proposed PD. We concentrate on hardware realization of the PD's memoryless nonlinearity part, as hardware realization of the linear filter \mathbf{g} is standard. We note that the amplitude gain function (34) has a natural pipeline processing structure. We only need to examine the case of $r^2 \leq A_{\max}^2$ as, for $r^2 > A_{\max}^2$, $P(r) = 1$. Let us first define the coefficients

$$f_i = \frac{2a_i}{\alpha_a}, \quad 1 \leq i \leq N_t, \quad (39)$$

and the variable

$$u = \frac{4\beta_a}{\alpha_a^2} \cdot r^2. \quad (40)$$

Then $\hat{P}(r)$ can be expressed as

$$\hat{P}(r) = \sum_{i=1}^{N_t} f_i u^{i-1} = \hat{P}^{(N_t)}(r), \quad (41)$$

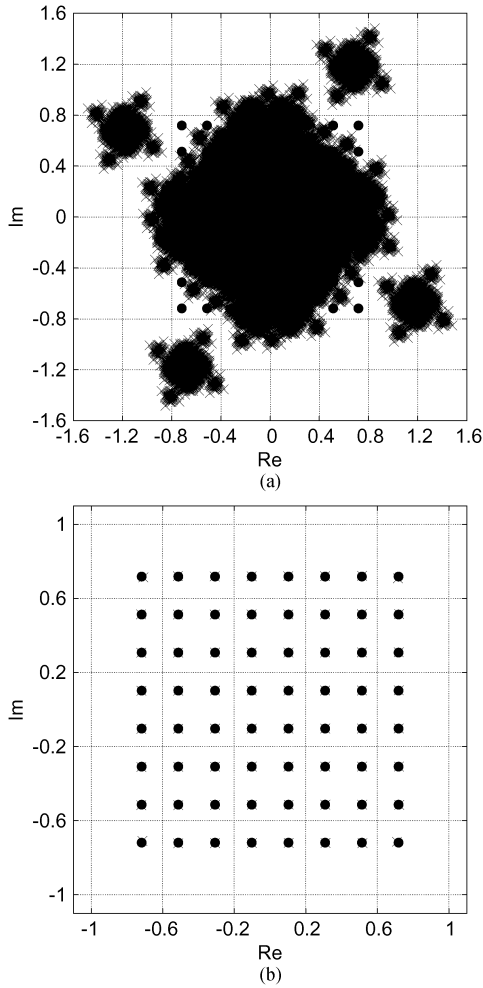


Fig. 9. Sixty-four-QAM signal, marked by •, (a) after the proposed PD, marked by ×, and (b) after the combined PD and Wiener HPA, marked by ×, where the Wiener HPA is specified by the parameter vector (12) with IBO = 5 dB, while the PD is designed based on the estimated parameter vector (43).

with the recursion for $\hat{P}^{(m)}(r)$, $1 \leq m \leq N_t$, given by

$$\hat{P}^{(m)}(r) = \begin{cases} f_{N_t}, & m = 1, \\ f_{N_t+1-m} + u \cdot \hat{P}^{(m-1)}(r), & 2 \leq m \leq N_t. \end{cases} \quad (42)$$

The recursive expression (42) for $\hat{P}(r)$ provides an effective VLSI structure for hardware realization of the memoryless non-linearity of the proposed PD defined by (38) and (30).

The VLSI structure of the proposed PD shown in Fig. 6 contains three parts. Part A implements the amplitude gain function $P(r)$ and part B realizes the phase predistortion function $\Omega(r)$, while part C is for the realization of the linear filter of the proposed PD. Most of the computation costs are for computing the amplitude gain function. The hardware realization of $\hat{P}(r)$, as depicted in part A.1 of Fig. 6, shows that the computation of $\hat{P}(r)$ requires only N_t multiplications and $N_t - 1$ additions. The advantage of this structure is that data is processed with an efficient pipeline. Additionally, multiplication units given in part A.1 of Fig. 6 can process data in a parallel fashion. The piecewise linear error compensation term $\hat{\varepsilon}(r^2)$ is illustrated in part A.2 of Fig. 6, which is only entered if $r^2 > \bar{R}_0^2$. Table I analyses the on-line complexity for computing the memoryless

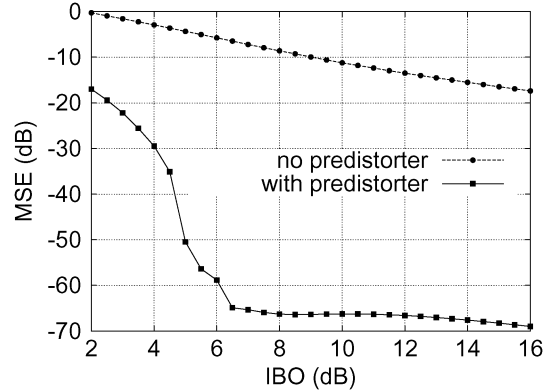


Fig. 10. MSE versus IBO performance, where the Wiener HPA is specified by the parameter vector (12), while the PD is designed based on the estimated parameter vector (43).

nonlinear predistortion of the proposed PD design. The appropriate choice for the order of Taylor expansion is $N_t = 7$ to 9. Therefore, the proposed PD design has a very low on-line computational complexity.

IV. SIMULATION STUDY

We considered the single-carrier 64-QAM system with the static nonlinearity of the memory HPA described by (6) and (7). The parameters of the memory HPA were given in (12).

A. PSO Based Identification Results

We first demonstrated the effectiveness of the PSO algorithm, presented in Section II-B, for the identification of the Wiener HPA model. The 64-QAM training set contained $K = 500$ data samples. With the swarm size $S = 20$ and the number of iterations $L_{\max} = 80$, Fig. 7 depicts the evolution of the MSE cost (16), normalized by the average 64-QAM symbol power $E[|x(k)|^2]$, for the cases of the measurement noise standard deviation $\sigma_\mu = 0.0$ and $\sigma_\mu = 0.01$, respectively, where the results were averaged over 100 runs. The identification results using the PSO are summarized in Table II. Fig. 8 compares the true amplitude and phase response of the Wiener HPA with those of the estimated Wiener HPA model given by

$$\begin{aligned} \hat{\mathbf{h}}^T &= [0.77065 \quad 0.15413 \quad 0.07721], \\ \hat{\mathbf{t}}^T &= [2.15917 \quad 1.16780 \quad 3.97040 \quad 2.06925]. \end{aligned} \quad (43)$$

The results obtained show that an accurate Wiener HPA model can be effectively identified using the PSO algorithm.

B. Proposed Predistorter Performance

We employed the estimated Wiener HPA model (43) to design the PD as detailed in Section III. The length of the linear filter for the PD was set to $N_g = 7$, while a Taylor expansion order $N_t = 9$ and a $Q = 5$ -piecewise linear interpretation were adopted for computing the amplitude gain function of the PD. The achievable performance of the designed PD was assessed using the MSE metric defined by

$$\text{MSE} = 10 \log_{10} \left(\frac{1}{K_{\text{test}}} \sum_{k=1}^{K_{\text{test}}} |x(k) - y(k)|^2 \right), \quad (44)$$

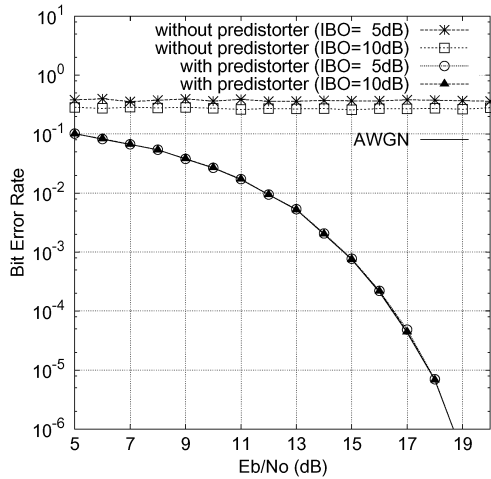


Fig. 11. BER versus SNR performance, where the Wiener HPA is specified by the parameter vector (12), while the PD is designed based on the estimated parameter vector (43).

as well as the system's BER, where K_{test} was the total number of test data, $x(k)$ was the input signal and $y(k)$ was the output of the combined PD and memory HPA system. The channel signal to noise ratio (SNR) was given by

$$\text{SNR} = 10 \log_{10} (E_b/N_o), \quad (45)$$

where E_b was defined as the energy per bit and N_o the power of the channel's additive white Gaussian noise (AWGN).

The output signal constellations after the designed PD and after the combined PD and Wiener HPA system are depicted in Fig. 9 for the value of IBO = 5 dB. It can be seen that even for IBO = 5 dB, the proposed PD can almost completely cancel out the nonlinear distortions and memory effects of the Wiener HPA. This is significant as the memory HPA is operating into the saturation region of $r^2 > r_{\text{sat}}^2$ for the peak input amplitude in the case of IBO = 5 dB, see Fig. 2. $K_{\text{test}} = 2 \times 10^5$ 64-QAM data were passed through the combined PD and Wiener HPA system to compute the MSE (44), and the resulting MSE as the function of IBO is plotted in Fig. 10.

The output signal after the memory HPA was then transmitted over the AWGN channel, and the BER was then determined at the receiver. The results so obtained are plotted in Fig. 11, in comparison with the benchmark BER curve of the ideal AWGN channel. It can be seen from Fig. 11 that the BER performance of the combined PD and HPA system is practically indistinguishable from those of the ideal AWGN channel even under the operating condition of IBO = 5 dB, which again demonstrates the effectiveness of the proposed PD design. The achievable BER performance of the combined PD and Wiener HPA system are further illustrated in Fig. 12 for the three values of the channel SNR.

V. CONCLUSION

An novel digital predistorter design has been proposed to compensate the distortions caused by Wiener memory HPAs which exhibit true output saturation characteristics. An efficient

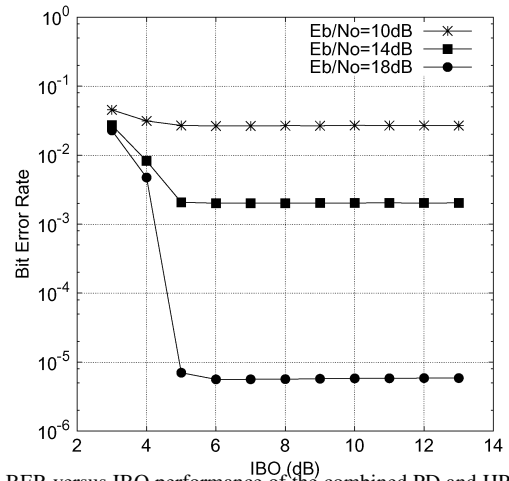


Fig. 12. BER versus IBO performance of the combined PD and HPA system, where the Wiener HPA is specified by the parameter vector (12), while the PD is designed based on the estimated parameter vector (43).

PSO based identification algorithm has been employed to estimate an accurate memory HPA model, based on which an algebraic PD solution can be directly obtained. It has been shown that the proposed PD design enjoys several important advantages, including a natural pipeline data processing structure suitable for simple VLSI hardware realization and low on-line computational complexity. The effectiveness of the proposed PD design has been illustrated by simulation results. In particular, it has been shown that this novel digital PD is capable of successfully compensating serious nonlinear distortions caused by the memory HPA operating into the output saturation region.

REFERENCES

- [1] L. Hanzo, S. X. Ng, T. Keller, and W. Webb, *Quadrature Amplitude Modulation: From Basics to Adaptive Trellis-Coded, Turbo-Equalised and Space-Time Coded OFDM, CDMA and MC-CDMA Systems*. Chichester, UK: John Wiley, 2004.
- [2] L. Hanzo, M. Münster, B. J. Choi, and T. Keller, *OFDM and MC-CDMA for Broadband Multi-User Communications, WLANs and Broadcasting*. Chichester, UK: John Wiley, 2003.
- [3] J. H. K. Vuolevi, T. Rahkonen, and J. P. A. Manninen, "Measurement technique for characterizing memory effects in RF power amplifiers," *IEEE Trans. Microwave Theory and Techniques*, vol. 49, no. 8, pp. 1383–1389, Aug. 2001.
- [4] C.-H. Lin, H.-H. Chen, Y.-Y. Wang, and J.-T. Chen, "Dynamically optimum lookup-table spacing for power amplifier predistortion linearization," *IEEE Trans. Microwave Theory and Techniques*, vol. 54, no. 5, pp. 2118–2127, May 2006.
- [5] B. Ai, Z.-Y. Yang, C.-P. Pan, S.-G. Tang, and T. T. Zhang, "Analysis on LUT based predistortion method for HPA with memory," *IEEE Trans. Broadcasting*, vol. 53, no. 1, pp. 127–131, Mar. 2007.
- [6] P. Jardin and G. Baudoin, "Filter lookup table method for power amplifier linearization," *IEEE Trans. Vehicular Technology*, vol. 56, no. 3, pp. 1076–1087, May 2007.
- [7] H.-H. Chen, C.-H. Lin, P.-C. Huang, and J.-T. Chen, "Joint polynomial and look-up-table predistortion power amplifier linearization," *IEEE Trans. Circuits and Systems II: Express Briefs*, vol. 53, no. 8, pp. 612–616, Aug. 2006.
- [8] R. Raich, H. Qian, and G. T. Zhou, "Orthogonal polynomials for power amplifier modeling and predistorter design," *IEEE Trans. Vehicular Technology*, vol. 53, no. 5, pp. 1468–1479, Sep. 2004.
- [9] D. R. Morgan, Z.-X. Ma, J. Kim, M. G. Zierdt, and J. Pastalan, "A generalized memory polynomial model for digital predistortion of RF power amplifiers," *IEEE Trans. Signal Processing*, vol. 54, no. 10, pp. 3852–3860, Oct. 2006.
- [10] L. Ding, G. T. Zhou, D. R. Morgan, Z. Ma, J. S. Kenney, J. Kim, and C. R. Giardina, "A robust digital baseband predistorter constructed using memory polynomials," *IEEE Trans. Communications*, vol. 52, no. 1, pp. 159–165, Jan. 2004.

- [11] M.-C. Chiu, C.-H. Zeng, and M.-C. Liu, "Predistorter based on frequency domain estimation for compensation of nonlinear distortion in OFDM systems," *IEEE Trans. Vehicular Technology*, vol. 57, no. 2, pp. 882–892, Mar. 2008.
- [12] L. Xu, X. Wu, M. Zhang, G. Kang, and P. Zhang, "A stable recursive algorithm for memory polynomial predistorter," in *Proc. MILCOM 2007*, Orlando, Florida, Oct. 29–31, 2007, pp. 1–5.
- [13] Y. Qian and T. Yao, "Structure for adaptive predistortion suitable for efficient adaptive algorithm application," *Electronics Letters*, vol. 38, no. 21, pp. 1282–1283, Oct. 2002.
- [14] D. Zhou and V. E. DeBrunner, "Novel adaptive nonlinear predistorters based on the direct learning algorithm," *IEEE Trans. Signal Processing*, vol. 55, no. 1, pp. 120–133, Jan. 2007.
- [15] S. Choi, E.-R. Jeong, and Y. H. Lee, "Adaptive predistortion with direct learning based on piecewise linear approximation of amplifier nonlinearity," *IEEE J. Selected Topics in Signal Processing*, vol. 3, no. 3, pp. 397–404, Jun. 2009.
- [16] V. P. G. Jiménez, Y. Jabrane, A. G. Armada, and B. Ait Es Said, "High power amplifier pre-distorter based on neural-fuzzy systems for OFDM signals," *IEEE Trans. Broadcasting*, vol. 57, no. 1, pp. 149–158, Mar. 2011.
- [17] Y. Wang, L. Xie, Z. Wang, H. Chen, and K. Wang, "An efficient algebraic predistorter for compensating the nonlinearity of memory amplifiers," in *Proc. 2010 IEEE Int. Conf. Communications, Circuits and Systems*, Chengdu, China, Jul. 28–30, 2010, pp. 800–804.
- [18] C. J. Clark, G. Chrisikos, M. S. Muha, A. A. Moulthrop, and C. P. Silva, "Time-domain envelope measurement technique with application to wideband power amplifier modeling," *IEEE Trans. Microwave Theory and Techniques*, vol. 46, no. 12, pp. 2531–2540, Dec. 1998.
- [19] A. A. M. Saleh, "Frequency-independent and frequency-dependent nonlinear models of TWT amplifiers," *IEEE Trans. Communications*, vol. COM-29, no. 11, pp. 1715–1720, Nov. 1981.
- [20] J. Kennedy and R. C. Eberhart, "Particle swarm optimization," in *Proc. 1995 IEEE Int. Conf. Neural Networks*, Perth, Australia, Nov. 27–Dec. 1 1995, pp. 1942–1948.
- [21] J. Kennedy and R. C. Eberhart, *Swarm Intelligence*. San Mateo, CA: Morgan Kaufmann, 2001.
- [22] A. Ratnaweera and S. K. Halgamuge, "Self-organizing hierarchical particle swarm optimizer with time-varying acceleration coefficients," *IEEE Trans. Evolutionary Computation*, vol. 8, no. 3, pp. 240–255, Jun. 2004.
- [23] S. M. Guru, S. K. Halgamuge, and S. Fernando, "Particle swarm optimisers for cluster formation in wireless sensor networks," in *Proc. 2005 Int. Conf. Intelligent Sensors, Sensor Networks and Information Processing*, Melbourne, Australia, Dec. 5–8, 2005, pp. 319–324.
- [24] W.-F. Leong and G. G. Yen, "PSO-based multiobjective optimization with dynamic population size and adaptive local archives," *IEEE Trans. Systems, Man, and Cybernetics, Part B*, vol. 38, no. 5, pp. 1270–1293, Oct. 2008.
- [25] S. Chen, X. Hong, B. L. Luk, and C. J. Harris, "Non-linear system identification using particle swarm optimisation tuned radial basis function models," *Int. J. Bio-Inspired Computation*, vol. 1, no. 4, pp. 246–258, 2009.
- [26] M. Ramezani, M.-R. Haghifam, C. Singh, H. Seifi, and M. P. Moghaddam, "Determination of capacity benefit margin in multiarea power systems using particle swarm optimization," *IEEE Trans. Power Systems*, vol. 24, no. 2, pp. 631–641, May 2009.
- [27] S. Chen, X. Hong, and C. J. Harris, "Particle swarm optimization aided orthogonal forward regression for unified data modelling," *IEEE Trans. Evolutionary Computation*, vol. 14, no. 4, pp. 477–499, Aug. 2010.
- [28] A. D. Kalafatis, L. Wang, and W. R. Cluett, "Identification of Wiener-type nonlinear systems in a noisy environment," *Int. J. Control*, vol. 66, no. 6, pp. 923–941, 1997.
- [29] A. Hagenblad, L. Ljung, and A. Wills, "Maximum likelihood identification of Wiener models," *Automatic*, vol. 44, no. 11, pp. 2697–2705, Nov. 2008.
- [30] F. M. Gardner, "Interpolation in digital modems. I. Fundamentals," *IEEE Trans. Communications*, vol. 41, no. 3, pp. 501–507, Mar. 1993.



Sheng Chen (M'90–SM'97–F'08) obtained his B.Eng. degree from the East China Petroleum Institute, Dongying, China, in January 1982, and his Ph.D. degree from the City University, London, in September 1986, both in control engineering. In 2005, he was awarded the Doctor of Sciences (D.Sc.) degree from the University of Southampton, Southampton, UK. From 1986 to 1999, He held research and academic appointments at the Universities of Sheffield, Edinburgh and Portsmouth, all in UK. Since 1999, he has been with the School

of Electronics and Computer Science, the University of Southampton, UK, where he currently holds the post of Professor in Intelligent Systems and Signal Processing. Dr Chen's recent research interests include adaptive signal processing, wireless communications, modeling and identification of nonlinear systems, neural network and machine learning, intelligent control system design, evolutionary computation methods and optimization. He has published over 450 research papers. In the database of the world's most highly cited researchers in various disciplines, compiled by Institute for Scientific Information (ISI) of the USA, Dr Chen is on the list of the highly cited researchers in the engineering category, see <http://www.ISIHighlyCited.com>.